PHILOSOPHICAL TRANSACTIONS OF THE ROYAL SOCIETY A MATHEMATICAL, PHYSICAL & ENGINEERING SCIENCES

Tension of Organizing Filaments of Scroll Waves

V. N. Biktashev, A. V. Holden and H. Zhang

Phil. Trans. R. Soc. Lond. A 1994 **347**, 611-630
doi: 10.1098/rsta.1994.0070

Tension of organizing filaments of scroll waves†

By V. N. Biktashev[1,2], A. V. Holden[2] and H. Zhang[2]

[1]*Institute of Mathematical Problems of Biology, Pushchino, Moscow Region, 142292, Russia*

[2]*Department of Physiology and Centre for Nonlinear Studies, University of Leeds, Leeds LS2 9JT, U.K.*

We consider the asymptotic theory for the dynamics of organizing filaments of three-dimensional scroll waves. For a generic autowave medium where two-dimensional vortices do not meander, we show that some of the coefficients of the evolution equation are always zero. This simpler evolution equation predicts a monotonic change of the total filament length with time, independently of initial conditions. Whether the filament will shrink or expand is determined by a single coefficient, the filament tension, that depends on the medium parameters. We illustrate the behaviour of scroll wave filaments with positive and negative tension by numerical experiments. In particular, we show that in the case of negative filament tension, the straight filament is unstable, and its evolution may lead to a multiplication of vortices.

1. Introduction

Winfree (1973) presented the first experimental images of three-dimensional autowave vortices (scroll waves) in the Belousov–Zhabotinsky reaction medium. Three-dimensional vortices in excitable media are generally non-stationary and move, in contrast to spiral waves in two-dimensional media, which are often stationary, or meander around a central region (Winfree 1991), and may be made to move by the influence of an external input (Davydov *et al.* 1988; Biktashev & Holden 1993, 1994) or an inhomogeneity (Ermakova & Pertsov 1988; Ermakova *et al.* 1989; Hramov *et al.* 1984; Pertsov & Ermakova 1988; Rudenko & Panfilov 1983).

Autowave vortices are believed to be the mechanism of some re-entrant cardiac arrhythmias and fibrillation; see the review by Janse (1991). The investigation of properties of three-dimensional vortices in excitable media provides insights into the possible behaviours of these processes in the cardiac tissue of animals whose heart wall is thick enough for three-dimensional effects to be significant. Krinsky *et al.* (1990, 1991) have reviewed the experimental evidence that the behaviour of vortices in human myocardial, in particular, ventricular tissue may be essentially three dimensional.

† This paper was produced from the authors' disk by using the TEX typesetting system.

Phil. Trans. R. Soc. Lond. A (1994) **347**, 611–630
Printed in Great Britain

A simple structure for exploring the dynamics of a vortex is that of vortex ring, in which the vortex filament is untorted and forms a circle. The symmetry of this structure allows its reduction to an effectively two-dimensional problem. Panfilov (1991) has reviewed his earlier works on the dynamics of a vortex ring with strong axial symmetry in a model of an excitable medium (Panfilov & Pertsov 1984; Panfilov & Rudenko 1987; Panfilov *et al.* 1986) . The ring radius changes with time and the ring shifts along the axis of symmetry, both with velocities that are inversely proportional to the current ring radius. The absolute values and sign of the coefficients of proportionality vary with the model parameters. The results of such phenomenological studies on vortex ring dynamics have been used to estimate the lifetime of vortex rings in mammalian myocardial tissue (Panfilov & Holden 1993).

Numerical experiments on three-dimensional autowave vortex dynamics have illustrated the richness of possible autowave vortex behaviour in three dimensions. As well as the evolution of a scroll ring mentioned above, some more examples of behaviours of the vortices have been described, including:

(i) A twisted scroll wave is unstable in a homogeneous medium and untwists, while a non-twisted scroll will develop a twist in an inhomogeneous medium. A twisted scroll has a shorter period than an untwisted one in the same medium (Panfilov *et al.* 1984).

(ii) At some values of the medium parameters, the ring filament can have a stable state, drifting with a constant radius (Brazhnik *et al.* 1988), or a stable steady state, in which it remains stationary with a constant radius (Nandapurkar & Winfree 1989; Courtemanche *et al.* 1990; Winfree 1990).

(iii) At some values of the parameters of the medium, vortices with self-knotted filaments may be stable or rigidly precessing (Winfree 1990).

(iv) Boundary influences can stabilize an initially drifting filament or change the direction of drift and contraction properties (Nandapurkar & Winfree 1989; Courtemanche *et al.* 1990).

(v) A filament may be pinned to a region of sharp inhomogeneity in the medium (Courtemanche *et al.* 1990; Vinson *et al.* 1993).

However, numerical simulations do not lead to general rules, and it always remains unclear how the behaviour will change as parameters and/or initial conditions are changed. To obtain the rules that determine vortex evolution we require some kind of theory that gives qualitative predictions for the vortex behaviour.

The development of an asymptotical theory for autowave vortex dynamics was begun by Yakushevich (1984), who derived the equations for filament motion for the very special case of the simplest auto-oscillatory medium with equal diffusion coefficients for all components. Keener (1988) has developed the asymptotical theory for reaction-diffusion systems of a more general form. This asymptotical theory is valid in the limit of characteristic scales of the filament that are much greater than the characteristic scale of a two-dimensional vortex. The strength of the theory lies in the possibility of considering motion of a one-dimensional object, the vortex filament, in three-dimensional space instead of the evolution of a three-dimensional distribution of several variables. This approach may be considered as an autowave analogue of the theory of hydrodynamic vortices developed by Da Rios (1906) (see Ricca 1991). This theory has been used for the analysis of the behaviour of helical filaments (Keener & Tyson 1990, 1991), and has been extended to strongly twisted vortices (Biktashev 1989*a*). For a special case of

PHILOSOPHICAL TRANSACTIONS OF THE ROYAL SOCIETY A MATHEMATICAL, PHYSICAL & ENGINEERING SCIENCES

Keener's equations, when the filament remains in the same plane, an integral invariant law (Panfilov *et al.* 1989) was found, which claims that the area of the region bounded by such a filament changes with constant speed.

In this paper we examine one particular consequence of Keener's theory, and introduce the filament tension as a property of a particular autowave medium. The filament tension coincides numerically with the proportionality coefficient between the reciprocal of the vortex radius and the rate of radial growth for an untwisted circular filament. The sign of the tension determines the principal macroscopic properties of vortices in an excitable medium. The behaviour of filaments with positive and negative tensions is illustrated by numerical experiments with the cubic FitzHugh–Nagumo equations in the form proposed by Winfree (1991).

2. The theory of filament dynamics

Since Keener's paper (1988) is well known, there is no need to repeat the details of the derivation of the evolution equation. Here we only briefly recapitulate key concepts of the theory, to introduce the terms that will be used in present paper and make the exposition self-consistent. The autowave medium is assumed to be described by a 'reaction-diffusion' system of partial differential equations of the generic form

$$\partial_t u = \boldsymbol{D}\Delta_3 u + f(u), \tag{2.1}$$

where $u = u(\boldsymbol{r}, t)$ is a vector-valued function of time and space, $u \in \boldsymbol{R}^l$, of dynamic variables (e.g. chemical species concentrations, or voltage and gating variables in cardiac tissue), $f(u) \in \boldsymbol{R}^l$ is the vector of reaction rates or ionic currents; $\boldsymbol{D} = \{D_{ij}\}$ is the diagonal matrix of diffusion coefficients (only one of which is non-zero for cardiac tissue, and which are all approximately equal for the Belousov–Zhabotinsky reaction medium), $\boldsymbol{r} \in \boldsymbol{R}^3$, and $\Delta_3 = \partial_x^2 + \partial_y^2 + \partial_z^2$ is the laplacian operator in three dimensions. The symbol ∂ is used here and below to denote partial differentiation by the subscripted variable.

The only assumptions on the properties of system (2.1) are that it has the two-dimensional solution (i.e. independent of one spatial dimensions, say, z) in the form of a stationary rotating vortex

$$u = V(r, \vartheta - \omega t), \tag{2.2}$$

where r, ϑ are polar coordinates in the (x, y) plane, ω is the rotation frequency of the spiral wave, and V is 2π-periodic with respect to ϑ, and that this solution is asymptotically stable, up to the natural invariance due to space and time homogeneity.

Singular perturbation theory uses the linearization operator L about this solution, for the two-dimensional system:

$$Lu \equiv \partial_t u - \boldsymbol{D}\Delta_2 u - \boldsymbol{F}(V)u, \tag{2.3}$$

where $\boldsymbol{F}(V) = \partial_u f(u)\,|_{u=V}$ is the matrix of partial derivatives of the reaction terms taken at the solution (2.2). According to the requirement of physical stability of solution (2.2), it is assumed that the null-space of L is exactly three-dimensional, with the null-eigenvectors $V_x = \partial_x V, V_y = \partial_y V, V_\vartheta = \partial_\vartheta V$ corresponding to infinitesimal shifts of solution (2.2) in two directions in space and in

time (the shift in time is equivalent to an infinitesimal rotation of the solution in space).

The three-dimensional vortices are the solutions of (2.1) that are close to (2.2) in every cross-section perpendicular to a sufficiently smooth simple curve (of small curvature and torsion) and for a sufficiently large vicinity of this curve. This curve is called the vortex filament. The Frenet–Serret equations are used to introduce the local coordinates in the vicinity of the filament for each instant of time:

$$\frac{\mathrm{d}R}{\mathrm{d}s} = T; \quad \frac{\mathrm{d}T}{\mathrm{d}s} = kN; \quad \frac{\mathrm{d}N}{\mathrm{d}s} = -kT + \tau B; \quad \frac{\mathrm{d}B}{\mathrm{d}s} = -\tau N. \tag{2.4}$$

Here R is a point on the filament; T is the tangent, N the normal and B the binormal unit vectors at point R; k is curvature, τ torsion of the filament, s is the arc length parameter at the filament. The three-dimensional solutions to (2.1) are sought in the coordinates s, p, q (where p and q correspond to directions N and B respectively) and have the form

$$u(s,p,q,t) = V(r, \vartheta + \phi(s,t) - \omega t) + u_1, \tag{2.5}$$

where r, ϑ are polar coordinates in the (p,q) plane, V is the two-dimensional vortex solution given by (2.2), $\phi(s,t)$ is the vortex rotation phase that varies slowly with s and t, and u_1 is a correction expected to be uniformly small in space and time. Substitution of (2.5) into (2.1) and using (2.2)–(2.4) yields, as a linear approximation in u_1, the equation of the form

$$Lu_1 = F[V,R], \tag{2.6}$$

where the free term $F[V,R]$ contains the derivatives of $V(p,q,t)$ and $R(s,t)$. The conditions for the existence of bounded and asymptotically periodic in time solutions u_1 to (2.6) (the Fredholm alternative) require that F should be orthogonal to the null-space of the adjoint operator L^+ defined with respect to the natural inner product $(\ ,\ )$ defined by

$$(u(x,y,t), v(x,y,t)) = \int_0^P \langle u(x,y,t), v(x,y,t)\rangle \,\mathrm{d}t, \tag{2.7}$$

where $P = 2\pi/\omega$ is the period of the vortex and the inner product $\langle\ ,\ \rangle$ includes integration over a disc of a large radius $\hat{r}$ in the (x,y) plane centred at $(0,0)$

$$\langle u(x,y), v(x,y)\rangle = \int_0^{2\pi} \mathrm{d}\vartheta \int_0^{\hat{r}} u(x,y)\cdot v(x,y) r \,\mathrm{d}r. \tag{2.8}$$

Here the dot denotes usual scalar product in $\boldsymbol{C}^l$ (the form of this inner product and the reason for the cut-off parameter $\hat{r}$ are discussed in § 6). This adjoint operator can be written as

$$L^+ v \equiv \partial_t v + \boldsymbol{D}_2 \Delta v + \boldsymbol{F}^{\mathrm{T}}(V) v. \tag{2.9}$$

We do not discuss the properties of L^+ here (in fact this is not a very straightforward problem); but assume that it also has an exactly three-dimensional null-space. The corresponding eigenvectors Y_x, Y_y, Y_ϑ are chosen biorthogonal to V_x, V_y, V_ϑ. The solvability conditions just yield the evolution equations for the filament position and phase distribution of the three-dimensional vortex of the form

$$\partial_t \phi = \partial_t N + (\partial_t R \cdot T)(\partial_s \phi - \tau) + b_1(\partial_s^2 \phi - \partial_s \tau) + a_1(\partial_s \phi - \tau)^2 - c_1 k, \tag{2.10}$$

$$(\partial_t R \cdot N) = b_2 k - c_2(\partial_s^2 \phi - \partial_s \tau) - a_2(\partial_s \phi - \tau)^2, \tag{2.11}$$

$$(\partial_t R \cdot B) = c_3 k - c_4(\partial_s^2 \phi - \partial_s \tau) - a_3(\partial_s \phi - \tau)^2, \tag{2.12}$$

where the coefficients are given by the inner products:

$$a_1 = (\boldsymbol{D}\partial_\vartheta^2 V, Y_\vartheta), \quad a_2 = (\boldsymbol{D}\partial_\vartheta^2 V, Y_x), \tag{2.13}$$

$$a_3 = (\boldsymbol{D}\partial_\vartheta^2 V, Y_y), \tag{2.14}$$

$$b_1 = (\boldsymbol{D}\partial_\vartheta V, Y_\vartheta), \quad b_2 = (\boldsymbol{D}\partial_x V, Y_x), \tag{2.15}$$

$$c_1 = (\boldsymbol{D}\partial_x V, Y_\vartheta), \quad c_2 = (\boldsymbol{D}\partial_\vartheta V, Y_x), \tag{2.16}$$

$$c_3 = (\boldsymbol{D}\partial_x V, Y_y), \quad c_4 = (\boldsymbol{D}\partial_\vartheta V, Y_y). \tag{2.17}$$

Keener assumed that the asymptotic orders of quantities in (2.10)–(2.12) are: τ, $\phi_s = \mathcal{O}(\epsilon)$ and R_t, ϕ_t, ϕ_{ss}, τ_s, $k = \mathcal{O}(\epsilon^2)$, so u_1 in (2.5) is also $\mathcal{O}(\epsilon^2)$. Then all the terms kept in (2.10)–(2.12) are of the order of ϵ^2.

The asymptotic assumptions are fulfilled for those specific solutions considered by Keener (1988) but it is difficult to find a reasonably general form of solutions that obey them. For example, almost all of these assumptions will be fulfilled if $R = \epsilon^{-2}\tilde{R}(\epsilon^2 s, \epsilon^4 t)$, $\phi = \tilde{\phi}(\epsilon s, \epsilon^2 t)$, except for τ, τ_s, which are $\tau \cong \epsilon^4$ and $\tau_s \cong \epsilon^6$. If we assume equal smoothness for R and ϕ, i.e. $R = \epsilon^{-1}\tilde{R}(\epsilon s, \epsilon^2 t)$, $\phi = \tilde{\phi}(\epsilon s, \epsilon t)$, then in the order $\mathcal{O}(\epsilon)$ we immediately proceed to the filament motion equation (3.27)–(3.28), as the other terms are of the order $\mathcal{O}(\epsilon^2)$.

The equations (2.10)–(2.12) together with the definitions (2.13)–(2.17) yield the asymptotic equations of motion for the three-dimensional autowave vortex, as obtained by Keener (1988).

In fact, the definitions (2.13)–(2.17) are not used in practice (except for the simplest case of equal diffusion coefficients, i.e. a scalar matrix $\boldsymbol{D}$), as their use would need the explicit solution of the adjoint linearized problem to find Y_x, Y_y, Y_ϑ either analytically or numerically, and it is simpler to fit these coefficients to the results of numerical simulations. The equations (2.10)–(2.12) have been used to construct some partial solutions, without knowing specific values of the coefficients, by Keener (1988) and Keener & Tyson (1988, 1990, 1991).

3. Some coefficients of the motion equations vanish

As we mentioned above, the null-eigenfunctions of L may be explicitly written

$$V_x = \partial_x V(r, \vartheta - \omega t) = \partial_r V(r, \vartheta - \omega t)\cos(\vartheta) - \frac{1}{r}\partial_\xi V(r, \vartheta - \omega t)\sin(\vartheta), \tag{3.1}$$

$$V_y = \partial_y V(r, \vartheta - \omega t) = \partial_r V(r, \vartheta - \omega t)\sin(\vartheta) + \frac{1}{r}\partial_\xi V(r, \vartheta - \omega t)\cos(\vartheta), \tag{3.2}$$

$$V_\vartheta = \partial_\vartheta V(r, \vartheta - \omega t) = \partial_\xi V(r, \vartheta - \omega t). \tag{3.3}$$

In general, the eigenfunctions of the adjoint problem cannot be written explicitly, and so it is impossible to find the coefficients (2.13)–(2.17) analytically. However, considering the symmetry of the problem leads to useful conclusions. In particular we consider the specific dependence of the unperturbed solution (2.2) on t and ϑ, i.e. its dependence only on the linear combination $\xi = \vartheta - \omega t$. This is simpler

if we change to a rotating coordinate system $t \to \tilde{t}$, $r \to \rho$, $\vartheta \to \xi$:

$$\tilde{t} = t; \quad \xi = \vartheta - \omega t; \quad \rho = r. \tag{3.4}$$

In these variables, the equations for the null-eigenfunctions of L, L^+ become

$$\tilde{L}\tilde{u} = \partial_\tau \tilde{u} - \omega \partial_\xi \tilde{u} - \tilde{\Delta}_2 \tilde{u} - \boldsymbol{F}(V(\rho,\xi))\tilde{u} = \partial_\tau \tilde{u} - \tilde{M}\tilde{u} = 0, \tag{3.5}$$

$$\tilde{L}^+\tilde{v} = \partial_\tau \tilde{v} - \omega \partial_\xi \tilde{v} + \tilde{\Delta}_2 \tilde{v} + \boldsymbol{F}^{\mathrm{T}}(V(\rho,\xi))\tilde{v} = \partial_\tau \tilde{v} + \tilde{M}^+\tilde{v} = 0, \tag{3.6}$$

where the operators $\tilde{M}$, $\tilde{M}^+$ do not depend on t and $\tilde{M}^+$ is adjoint to $\tilde{M}$ with respect to the inner product $\langle\ ,\ \rangle$ in the (ρ,ξ) plane. Here and below the tilde denotes objects considered in the rotating coordinate system (i.e. functions depending on ρ, ξ, $\tilde{t}$ instead of r, ϑ, t). The null-eigenfunctions (3.1)–(3.3) may be represented in this new variables as

$$\tilde{V}_x = \mathrm{Re}\{\mathrm{e}^{\mathrm{i}\omega\tau}\tilde{V}_+(\rho,\xi)\}, \tag{3.7}$$

$$\tilde{V}_y = \mathrm{Im}\{\mathrm{e}^{\mathrm{i}\omega\tau}\tilde{V}_+(\rho,\xi)\}, \tag{3.8}$$

$$\tilde{V}_\vartheta = \tilde{V}_0(\rho,\xi), \tag{3.9}$$

where we denote

$$\tilde{V}_0(\rho,\xi) = \partial_\xi V(\rho,\xi), \tag{3.10}$$

$$\tilde{V}_+(\rho,\xi) = \mathrm{e}^{\mathrm{i}\xi}(\partial_\xi V(\rho,\xi) + (\mathrm{i}/\rho)\partial_\xi V(\rho,\xi)). \tag{3.11}$$

Comparison of equation (3.5) and the expressions (3.7)–(3.9) shows that the (time-independent) operator $\tilde{M}$ considered on the space of functions of ρ, ξ (but not $\tilde{t}$) has a spectrum on the imaginary axis consisting of points 0, $\mathrm{i}\omega$ and $-\mathrm{i}\omega$, with the corresponding eigenfunctions $\tilde{V}_0$, $\tilde{V}_+$ and $\tilde{V}_- = \tilde{V}_+^*$.

In § 2 we assumed that the null-space of both L and also L^+ is three dimensional. This assumption requires that both equation (3.5) and (3.6) have a three-dimensional space of solutions bounded in time, which in turn implies that the operator $\tilde{M}^+$ has exactly three eigenvalues on the imaginary axis. Therefore these eigenvalues must coincide with those for $\tilde{M}$. Since $\tilde{M}^+$ is a real operator as well as $\tilde{M}$, its eigenfunctions must also have the form $\tilde{Y}_0$, $\tilde{Y}_+$ and $\tilde{Y}_- = \tilde{Y}_+^*$, while $\tilde{Y}_0$ is a real function. Therefore, we can conclude that the solutions to (3.6) should have the form

$$\tilde{Y}_x = \mathrm{Re}\{\mathrm{e}^{\mathrm{i}\omega\tau}\tilde{Y}_+(\rho,\xi)\}, \tag{3.12}$$

$$\tilde{Y}_y = \mathrm{Im}\{\mathrm{e}^{\mathrm{i}\omega\tau}\tilde{Y}_+(\rho,\xi)\}, \tag{3.13}$$

$$\tilde{Y}_\vartheta = \tilde{Y}_0(\rho,\xi). \tag{3.14}$$

If we define real-valued functions $\tilde{Y}_1$, $\tilde{Y}_2$ by

$$\tilde{Y}_+(\rho,\xi) = \mathrm{e}^{\mathrm{i}\omega\xi}(\tilde{Y}_1(\rho,\xi) + i\tilde{Y}_2(\rho,\xi)), \tag{3.15}$$

then we can obtain the expressions for the adjoint eigenfunctions in the original coordinates x, y (r, ϑ) completely analogous to (3.1)–(3.3):

$$Y_x = Y_1(r, \vartheta - \omega t)\cos(\vartheta) - Y_2(r, \vartheta - \omega t)\sin(\vartheta), \tag{3.16}$$

$$Y_y = Y_1(r, \vartheta - \omega t)\sin(\vartheta) + Y_2(r, \vartheta - \omega t)\cos(\vartheta), \tag{3.17}$$

$$Y_\vartheta = Y_0(r, \vartheta - \omega t). \tag{3.18}$$

Nevertheless, to establish the desired properties of the coefficients (2.13)–(2.17), it is more convenient to treat the inner products (2.7) and (2.8) in the rotating coordinate system, where it has the form

$$(\tilde{u}(\rho,\xi,\tilde{t}), \tilde{v}(\rho,\xi,\tilde{t})) = \int_0^P \mathrm{d}\tilde{t} \int_0^{2\pi} \mathrm{d}\xi \int_0^{\hat{r}} \tilde{u}(\rho,\xi,\tilde{t})\tilde{v}(\rho,\xi,\tilde{t})\rho\,\mathrm{d}\rho, \tag{3.19}$$

for in these variables the dependence of both functional bases on $\tilde{t}$ is explicit. Now it is easy to see that the orthogonality conditions

$$(V_x, Y_x) = 1, \tag{3.20}$$

$$(V_y, Y_x) = 0 \tag{3.21}$$

necessitate

$$\mathrm{Re} \int_0^{2\pi} \mathrm{d}\xi \int_0^{\hat{r}} \tilde{V}_+(\rho,\xi)\tilde{Y}_-(\rho,\xi)\rho\,\mathrm{d}\rho = \frac{1}{\pi}, \tag{3.22}$$

$$\mathrm{Im} \int_0^{2\pi} \mathrm{d}\xi \int_0^{\hat{r}} \tilde{V}_+(\rho,\xi)\tilde{Y}_-(\rho,\xi)\rho\,\mathrm{d}\rho = 0. \tag{3.23}$$

Further the condition that

$$(V_x, Y_\vartheta) = 0 \tag{3.24}$$

is fulfilled automatically and does not necessitate any new requirements, due to the specific dependence on $\tilde{t}$, as the integration of the factor $\mathrm{e}^{\mathrm{i}\omega t}$ over the period vanishes.

In the same way, we can see that those of the inner products in (2.13)–(2.17) that include 'rotational' eigenfunctions on one side and 'shift' ones on the other, will also vanish. These are:

$$a_2 = a_3 = c_1 = c_2 = c_4 = 0. \tag{3.25}$$

This is the principal conclusion of this section. As a result, the system (2.10)–(2.12) obtains a simpler form

$$\partial_t\phi = \partial_t N + \partial_t R \cdot T(\partial_s\phi - \tau) + b_1(\partial_s^2\phi - \partial_s\tau) + a_1(\partial_s\phi - \tau)^2, \tag{3.26}$$

$$\partial_t R \cdot N = b_2 k, \tag{3.27}$$

$$\partial_t R \cdot B = c_3 k. \tag{3.28}$$

Note, that we have used the same assumptions to obtain (3.26)–(3.28) that were used for the derivation of (2.10)–(2.12). According to the remark at the end of § 2, the closed equations (3.27), (3.28) for the filament motion can be deduced without any symmetry considerations, in the case that R and ϕ are equally smooth functions, symbolically $\partial_s\phi/\phi \cong \partial_s R/R$. These equations are valid even if $\partial_s\phi/\phi \cong (\partial_s R/R)^{1/2}$, i.e. for relatively large twists. The symmetry arguments in this section, naturally, do not depend on the asymptotic assumptions, as they concern the expressions (2.10)–(2.17) independent of ϵ.

4. Tension of the filament

The important property of the system (3.26)–(3.28) with respect to (2.10)–(2.12) is that now the equations of motion for the filament position R (3.27)–(3.28) are independent of the distribution of the rotation phase ϕ. These two equations (3.27)–(3.28) can be combined together, if we recall the definitions of the unit vectors (2.4). The resulting equation can be written in the form

$$\partial_t R = b_2 \mathcal{D}_s^2 R + c_3 [\mathcal{D}_s R \times \mathcal{D}_s^2 R]. \tag{4.1}$$

This equation should be understood as an equation for vector function $R(\sigma, t)$ with a parameter σ chosen so that points with equal σ move orthogonally to the filament, and arbitrary in other respects (note that the arc length s may not obey this property). Then the arc length differentiation operator $\mathcal{D}_s$ is defined as

$$\mathcal{D}_s f(\sigma, t) \equiv \partial_\sigma f(\sigma, t) / \mid \partial_\sigma r(\sigma, t) \mid . \tag{4.2}$$

Such a choice of parameterization differs from that suggested in Keener (1988), which would be inconvenient for the purposes of the present paper.

Now let us consider the total length of the filament defined at each t:

$$S(t) \equiv \int \mathrm{d}s = \int \mid \partial_\sigma R(\sigma, t) \mid \, \mathrm{d}\sigma, \tag{4.3}$$

where the integral is taken over the whole filament. Direct calculations show that if the boundaries of the medium are smooth and impermeable (which implies that the filament always touches them normally), or the filament is closed, then, by the equation (4.1) the time derivative of functional (4.3) is

$$\frac{\mathrm{d}S}{\mathrm{d}t} = -b_2 \int \mid \mathcal{D}_s^2 R \mid^2 \, \mathrm{d}s = -b_2 \int k^2(s) \, \mathrm{d}s. \tag{4.4}$$

So, if the filament is not straight and $b_2 > 0$ then its total length diminishes in time irrespective of its initial form, provided the assumptions of the filament smoothness are fulfilled. Note that this statement depends only on the value of b_2 and does not depend on other coefficients of (3.26)–(3.28) including c_3.

In contrast, if $b_2 < 0$ (as in Panfilov & Rudenko (1987) and Panfilov *et al.* (1986)) then (4.1) appears to be ill-posed because its solutions do not depend continuously on the initial conditions, and even may not exist; it is easily seen by linearizing this equation at the straight filament. This property makes it is necessary to account for higher-order derivatives in s. If $\mid b_2 \mid$ is small enough, such a higher-order approximation could become well posed and keep its asymptotic sense, as it is the case in Kuramoto–Sivashinsky equation. However, it is well known that ill-posed equations of this kind with analytical initial conditions usually have unique solutions for some non-zero time interval. Along these solutions equation (4.1) determines the monotonic growth of the length until the applicability conditions for the asymptotical theory no longer hold.

So, we can summarize that the the coefficient b_2 plays a very special role in the dynamics of the filament. Its sign uniquely determines whether the length of the filament increases or decreases irrespective of the form of the filament and the values of the other parameters of the autowave medium, provided that the filament is a sufficiently smooth curve and the interaction of the filament with the boundaries, as well as the interaction of distant pieces of the same or

PHILOSOPHICAL TRANSACTIONS OF THE ROYAL SOCIETY A MATHEMATICAL, PHYSICAL & ENGINEERING SCIENCES

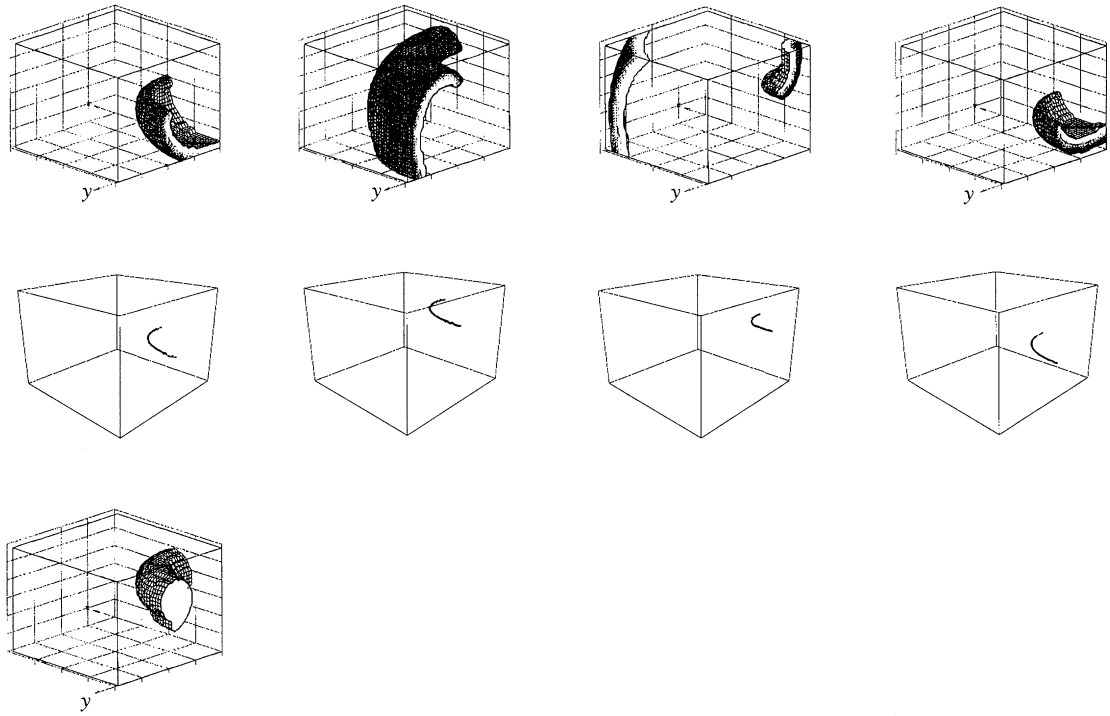

Figure 1. An illustration to the concepts of instant singular filament and inexcited core. Medium size is $120 \times 120 \times 90$ grid points ($60 \times 60 \times 45$ su). This figure is a piece of the experiment shown on figure 4 below. First row: the positions of the excitation wave in time instants 30, 45, 60, 75 tu (average period of this vortex is about 50 tu). Shown is the region with $u > u_*$, where u_* is -1.0 for this picture. The region is coloured depending on the value of v, greater values are lighter, so darker surface is the front of the wave, and lighter surface is back. Second row: the position of the singular filament, which is the line defined by equations $u = u_* = -1.0$ and $v = v_* = 0$, at the same time instants. Third row: the core of the vortex, i.e. the region not excited during this rotation of the vortex, u not exceeded $\bar{u}$ which is 1.0 for this picture.

different filaments can be neglected. Due to this property, the coefficient b_2 can be reasonably called the filament tension.

5. Numerical illustrations

Here we present some illustrations that the behaviour of filaments, extracted from numerical solutions of the partial differential excitation equation in $\boldsymbol{R}^3$, can be understood in terms of equations (3.26)–(3.28), and obeys the qualitative prediction (4.4), that the global behaviour of the filament is determined by the sign of b_2. If b_2 is positive, the filament will shorten; is b_2 is negative, the filament will lengthen – if the dynamics of the vortex is regular enough for the concept of filament to remain sensible, and the filament is neither too strongly curved nor influenced by boundaries (except at its ends if they touch the boundaries).

All numerical computations used the cubic FitzHugh–Nagumo system in $\boldsymbol{R}^3$, as described in the Appendix. The filament of a rigidly rotating straight scroll wave is clearly defined, as a line with constant values of the dynamic variables; since no such line exist for evolving vortex, an operational definition for the filament is

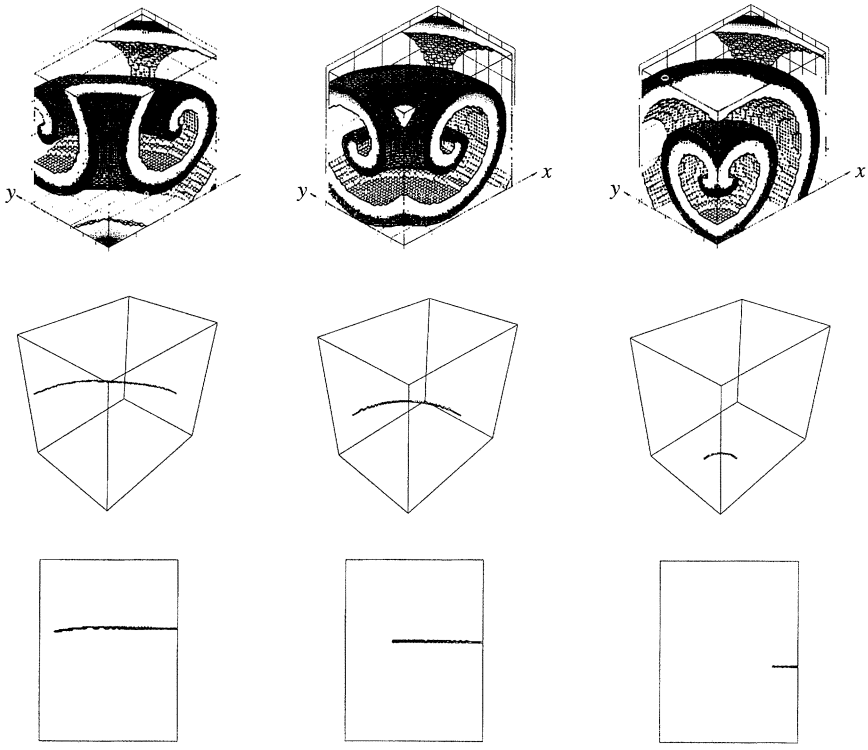

Figure 2. Collapsing vortex with positive tension. Parameters of the medium are $\epsilon = 0.3$, $\beta = 0.68$, $\gamma = 0.5$. Size of the array is $120 \times 90 \times 120$ grid points ($60 \times 45 \times 60$ su). The drawing parameters are $u_* = -1.2$ and $v_* = 0$. Upper row: the excitation wave. Second row: the singular filament. Third row: the singular filament, shown in projection to the y–z plane. First column: $t = 31.56$ tu, second rotation. Second column: $t = 340.11$ tu, 30th rotation. Third column: $t = 685.20$ tu, 61 st rotation.

needed. Two such definition used in our experiments are described in Appendix. They do not coincide but correlate well with each other when the evolution of the vortex is sufficiently slow. This is related to the fact that the filament is a virtual structure that, in the context of the present paper, is a consequence of the pattern of nonlinear wave activity in $\boldsymbol{R}^3$ and has only an asymptotical sense, rather than being a real physical object and a cause of such activity.

Figure 1 illustrates a segment of a scroll wave with a curved filament, and the two sorts of filaments extracted from this wave using the two different algorithms described in the Appendix. Here the 'thin filament' which is the cross-section of isosurfaces of the two dynamic variables at one instant in time, moves around the 'thick' filament, which is the region not invaded by the excitation during one revolution of the vortex.

The experiments were performed at two different parameter sets, one of which yielding positive tension of scroll wave filament, and the other negative. In both models, the two-dimensional vortices follow a rigid rotation and do not meander.

Figure 2 shows the evolution of the vortex with positive tension of the filament. The initial condition for this vortex was an almost straight filament touching adjacent borders of the medium. This vortex evolves to a quarter of a scroll ring

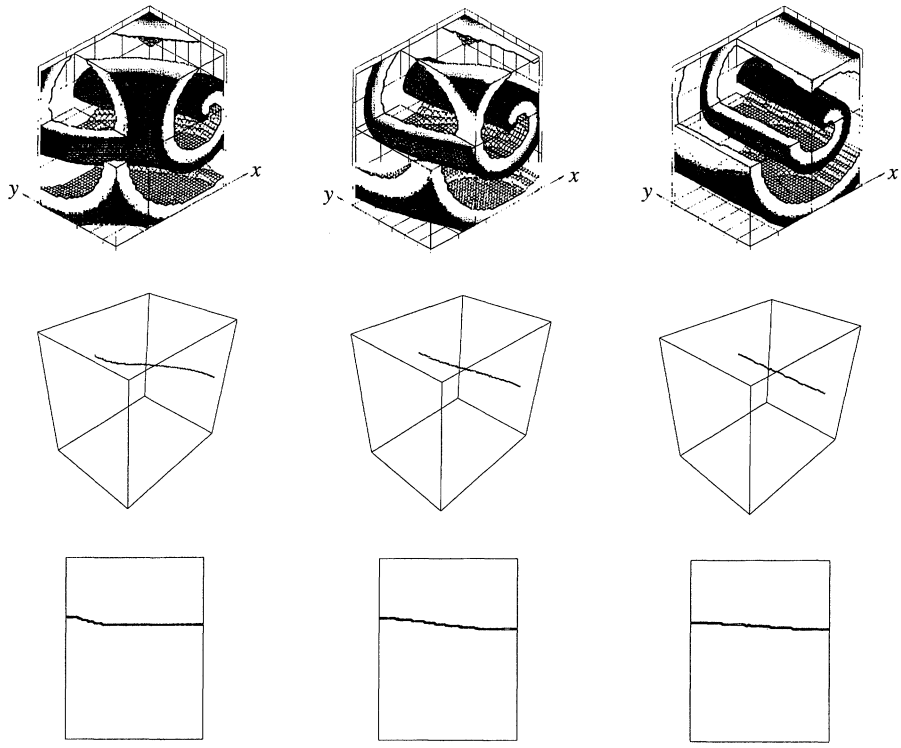

Figure 3. Straightening vortex with positive tension. Parameters and notations are same as in figure 2. A part of the medium is 'cut out' to show the 'internal' pattern which would be otherwise hidden by spreading out waves. The time moments chosen: 40.98 tu (three-dimensional rotation), 160.59 tu (14th rotation) and 419.82 tu (38th rotation).

with its centre at the rib of the box, and this scroll collapses towards this rib, and also shows a vertical drift. This example demonstrates that the axial symmetry of the collapsing vortex ring is stable, since in this case the vortex initially did not have this symmetry, but acquired it during the evolution.

Unlike the examples with the piecewise linear model considered by Panfilov & Rudenko (1987), and the predictions of the above theory, the vertical drift velocity is obviously not proportional to the horizontal drift velocity, but grows more rapidly at smaller radii of the ring. Thus, at this radii and in this medium, which is different from that studied by Panfilov & Rudenko (1987), the theory is no longer quantitatively valid. However, the qualitative prediction of a monotonic change of the filament length remains valid.

Different initial conditions in the same medium can lead to qualitatively different behaviour of the vortex, shown on figure 3. In this case, the filament initially touched opposite borders of the box.

Now the vortex could not collapse without an increase in the length of its filament, and this would contradict the prediction of the theory. Instead of collapsing, the vortex straightens, and the length of its filament tends to the thickness of the box. Note that the filament of this vortex does not remain planar during the evolution, due to the different vertical drift of its different pieces.

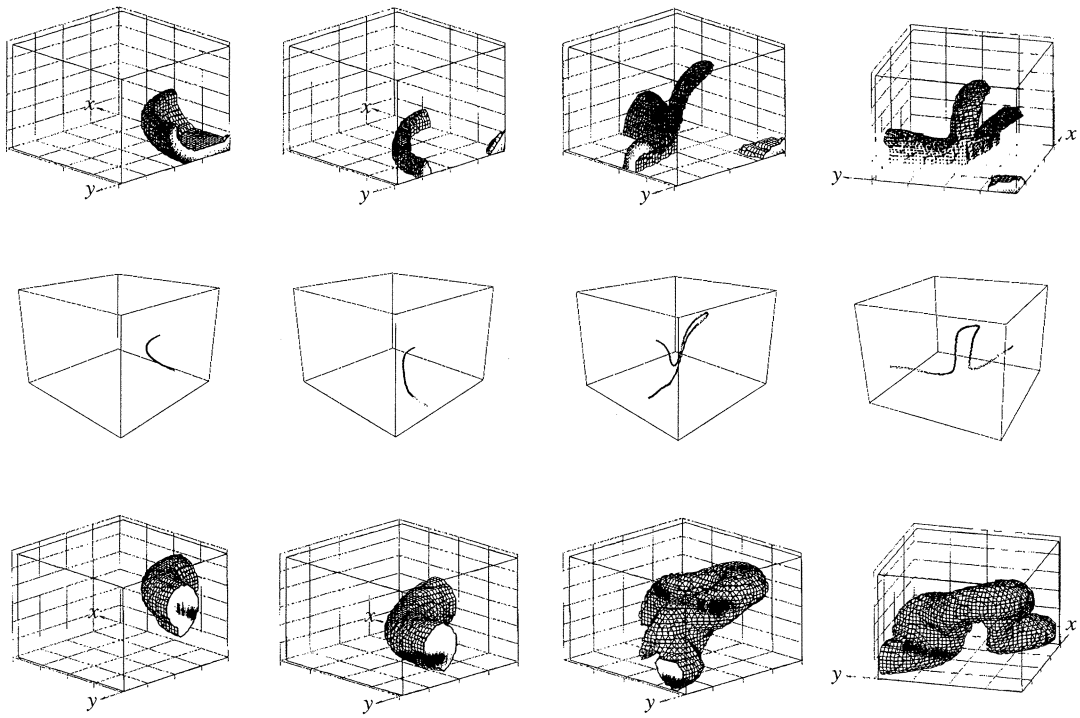

Figure 4. A quarter of a circular filament with negative tension ($\epsilon = 0.3$, $\beta = 0.8$, $\gamma = 0.5$). Medium size is $120 \times 120 \times 90$ grid points ($60 \times 60 \times 45$ su). The filament expands remaining circular and then deforms. Upper row: excitation wave. Second row: singular filament. Third row: the core of the vortex determined through a rotation preceding corresponding time instant on upper rows. Columns 1–3: times 77.94 tu (1st rotation), 278.34 tu (5th rotation), and 429.99 tu (8th rotation). Column 4: the same as column 3, from another point of view.

Panfilov & Rudenko (1987) observed expanding scroll rings at parameters in the piecewise-linear model that supported spiral waves with large cores; the larger the core, the larger the rate of expansion of the circular filament. Ermakova *et al.* (1986, 1989) showed that in this parameter region the interaction with boundaries is considerable, so a numerical demonstration of behaviour associated with a negative tension requires a large medium and long simulation time. Figure 4 shows the expansion and drift of a quarter of untwisted scroll ring and its interaction with a zero-flux boundary.

The scroll ring expands until it touches the bottom of the medium. Thereafter it loses its circular shape, deforms and breaks onto two pieces. This pieces are identical, due to the symmetry of the medium and of the initial conditions with respect to interchange of x and y coordinates.

The filament in such an expanding scroll ring is increasing in length and straightening, however a straight filament with a negative tension should be unstable, and this may provide the mechanism of the break of the scroll ring on figure 4. In the next experiment, we performed a direct check of the instability of the straight filament. With the same parameters as for figure 4*a* vortex with a straight, untwisted filament was initiated, which was perfectly independent of the z coordinate. Then this vortex was slightly perturbed, by applying a very small

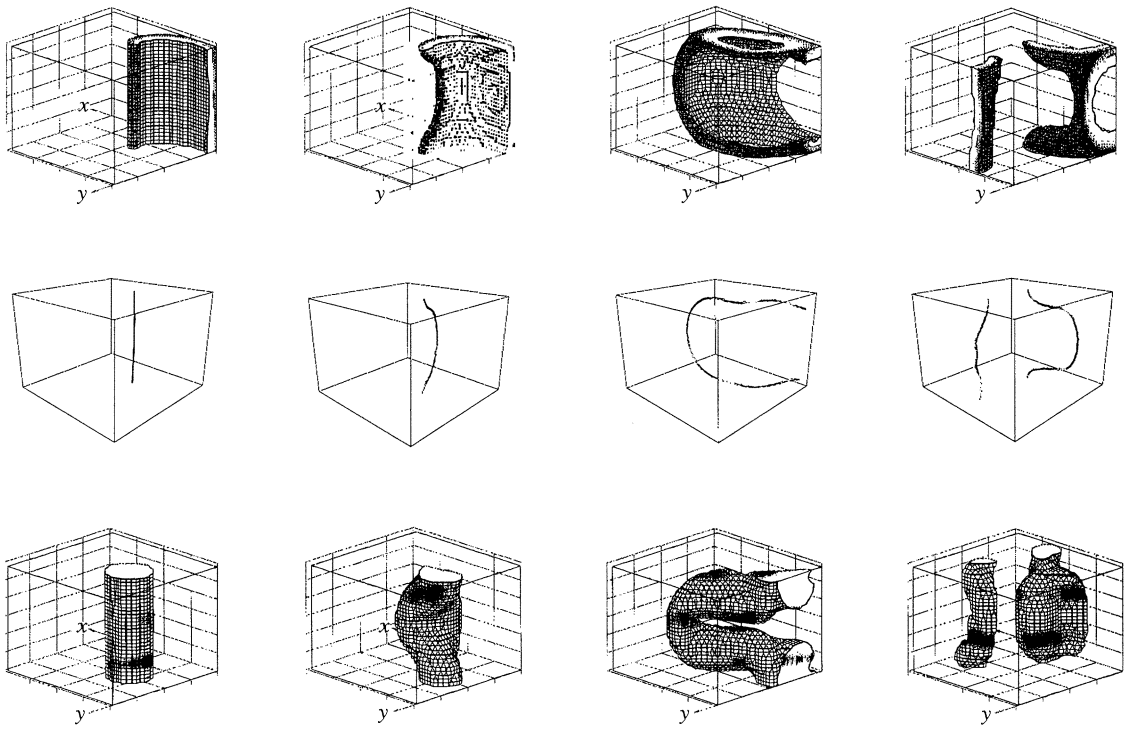

Figure 5. Instability of straight filament with positive tension. Parameters are same as in figure 4. Initially perfectly straight vortex (independent on the z coordinate), was slightly perturbed, by adding 0.0005 tu at all grid nodes $z = 22.5$ su and 0.001 at $z = 23$ su, during one computations step at $t = 90.0$ tu. Further evolution leads to curving of the vortex filament and then to its break onto two pieces. Shown are times 524.61 tu (9th rotation), 781.35 tu (14th rotation), 953.10 tu (17th rotation) and 1175.76 (21st rotation).

external stimulus depending on z. The perturbation was chosen so small that no changes in the behaviour of the vortex were visible during the following eight rotations. The subsequent evolution of the filament is illustrated in figure 5: the straight filament has responded to the perturbation by curving and extending.

Further evolution of the vortex in this experiment was rather complicated and included, as in the previous case, replication of vortices due the annihilation of a piece of filament at a border.

To check directly the prediction about monotonicity of the filament length, we measured this length during the evolution in the experiments presented at figures 2, 3 and 5. The length was estimated roughly by the number of grid cells the singular filament crosses. To hide the effect of the oscillations of the singular filament, we measured its length synchronously with rotation of the vortex. The results are shown on figure 6.

We can see that despite the rough estimation procedure for length and the illustrated behaviours are rather far from conditions for quantitative validity of the asymptotic theory, the quantitative behaviour obeys this theory pretty well. Note that in all cases the coefficient c_3 is significant and the filament is not planar, so the integral invariant law of Panfilov *et al.* (1989) is not applicable here.

PHILOSOPHICAL TRANSACTIONS OF THE ROYAL SOCIETY A MATHEMATICAL, PHYSICAL & ENGINEERING SCIENCES

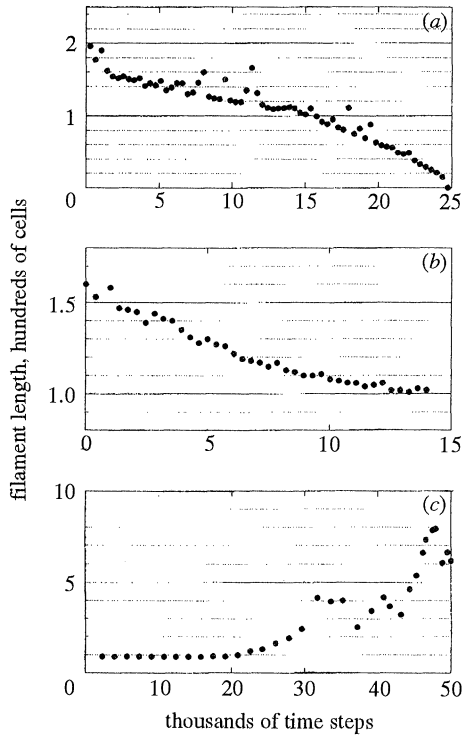

Figure 6. The length of the filament, estimated as the number of singular cell grids, against time measured in computation steps. Each point on a plot corresponds to a rotation period. (*a*) Positive tension, experiment shown on figure 2. Up to experimental errors caused by rough estimation procedure, the length monotonously decreases to zero. (*b*) Positive tension, experiment shown on figure 3. The length monotonously decreases to the thickness of the box. (*c*) Negative tension, experiment shown on figure 5. The first touching of the vortex filament to medium boundaries was at the time step 31770 = 953.10 tu, which was followed by the first violation of monotonous growth.

6. Discussion

The equation of motion for filament position (4.1) has been used without derivation by Panfilov *et al.* (1987) as its physical meaning is quite clear, unlike the system (2.10)–(2.12). This equation was also implicit in the statement in Brazhnik *et al.* (1988) that for a medium where a circular ring expands a straight filament should be unstable. In the present paper we have substantiated this physically obvious equation and have shown that

(1) the filament motion behaves as if each piece of the filament moves as a piece of a circular filament, and in leading terms this motion does not depend on the evolution of the phase,

(2) a monotonic change of the filament length takes place independently on the value of the coefficient c_3 determining the motion of a circular filament along its symmetry axis and independent of the current shape of the filament. Note that the effect of coefficient c_3 makes the evolution of the filament much more complicated, e.g. in general it makes impossible for an initially planar filament to remain planar.

The theoretical conclusions are made within the assumptions and limits of

Keener's approach and some open questions still remain. We have already mentioned that the problem of the the spectrum of the adjoint operator is not straightforward. At least, we have been unable to prove the property required (the dimension of the null-space of the adjoint operator) on the basis of the general assumptions used both here and by Keener.

Another open question is the meaning of the inner product (2.8) and the cut-off parameter $\tilde{r}$. Keener (1988) considered the limit $\hat{r} \to \infty$, and divided the resulting integral by the area of the disc $\pi\hat{r}^2$ assuming that both functions u and v are asymptotically periodic as $r \to \infty$. He presented heuristic arguments why the values of coefficients determined with such an inner product should converge to physically sensible values at an intermediate range of $\hat{r}$ that are greater than the two-dimensional characteristic lengths and less than the distance to the nearest shock structure caused by interaction of waves radiated by distant pieces of the filament.

The functions u are indeed asymptotically periodic, as they are constructed from the unperturbed solution V which is asymptotically periodic. However, there is no reason to assume the same property for the functions v from the adjoint space. From considering the definition (3.6) we can only expect that their dependence on r should have a form

$$v \cong \exp(\lambda r) ap(r), \tag{6.1}$$

where λ may be zero as well as positive or negative and ap denotes an asymptotically periodic function.

On the other hand, it is easy to see that the adjoint eigenfunctions defined by (3.6) are none other than the functions that determine the sensitivity of two-dimensional vortex position and phase to small perturbations, and hence sensitivity to slight inhomogeneities (see Biktashev & Holden 1994). As far as we are aware, these sensitivity functions have not yet been studied either numerically or analytically. There is indirect evidence that they rapidly drop with distance. Numerical experiments with vortices in stepwise inhomogeneous media (Panfilov & Vasiev 1991; Biktashev & Holden 1994) show that the vortex responds to the inhomogeneity only when it is fairly close. Ermakova *et al.* (1986, 1989) and Biktashev & Holden (1993, 1994) have demonstrated analogous effects with major inhomogeneities such as boundaries of the medium or the presence of other vortices. Biktashev (1989*b*) and then Pismen & Nepomnyashchy (1991, 1992) have shown that in the complex Ginzburg–Landau equation the interaction of vortex with boundaries drops exponentially with distance. If we assume that the sensitivity to such strong inhomogeneities as boundaries, should be qualitatively similar to the sensitivity to small perturbations, or accept the indirect evidences of numerical experiments mentioned above, then we should conclude that λ in (6.1) is negative.

If this hypothesis is true, then the integrals of the type (2.13)–(2.17) converge without any normalization. Then we can let $\hat{r}$ in (2.8) tend to infinity.

It is well known that the spectrum of an operator strongly depends upon the space in which this operator is considered. Since the space of perturbations is the space of functions bounded but not necessary vanishing at $r \to \infty$, the adjoint space may include only functions that are integrable over the whole plane, and the adjoint operator should be considered in this space. So, revealing the conditions when the adjoint operator has a three-dimensional null-space of functions of the

PHILOSOPHICAL TRANSACTIONS OF THE ROYAL SOCIETY A MATHEMATICAL, PHYSICAL & ENGINEERING SCIENCES

form (6.1) with $\lambda < 0$ would give more understanding to the mathematical nature of autowave vortices, and the reasons for their paradoxical property that the solution, although not localized itself, behaves as a localized object with respect to external influences. We believe this question remains unresolved, and that it has never been accurately formulated. We expect that these conditions should be related to the fact that the vortex is a source of waves, i.e. the group velocity of waves far from core is directed outward.

It is interesting to compare the motion of autowave vortex filament to that of hydrodynamic vortex. Note that the motion equations first obtained by Da Rios (1906) can be considered as a special case to (4.1), in spite of the fact that they describe other physical processes and are derived from other basic equations by different mathematical methods. Indeed, the equation (4.1) leads to the following system for curvature and torsion

$$\partial_t k = b_2 \mathcal{D}_s^2 k + k^3 - k\tau^2 - c_3 2\tau \mathcal{D}_s k + k\mathcal{D}_s \tau, \tag{6.2}$$

$$\partial_t \tau = b_2 2k^2 \tau + \mathcal{D}_s(2\tau \mathcal{D}_s k/k + \mathcal{D}_s \tau) + c_3 k \mathcal{D}_s k + \mathcal{D}_s(\mathcal{D}_s^2 k/k - \tau^2), \tag{6.3}$$

which at $b_2 = 0$, $c_3 = -1$, $\mathcal{D}_s \to \partial_s$ coincides with that given by Ricca (1992); due to conservation of arc length, the filament here can be parametrized by s. Conservation of the length of the filament of a hydrodynamic vortex is a well known result in hydrodynamics. Here we have one more example of analogy between dissipative and hamiltonian systems, when a quantity conserved in the latter case proves to be monotonically changing in the former. An interesting question arises, if this is only a formal analogy owing to the fact that there cannot be many simple equations describing smooth motion of a curve in three dimensions, or if the two kinds of vortices indeed have a similar mathematical nature.

There have been attempts to verify the dynamics equations (2.10)–(2.12) by numerical simulations of vortices with helical filaments (Henze *et al.* 1990; Keener & Tyson 1991). Keener & Tyson (1991) have found the values of some coefficients of (2.13)–(2.17) by matching the numerics of Henze *et al.* (1990) for Oregonator kinetics to the system (2.10)–(2.12). In particular, they have found the dimensionless ratio $a_2/(b_2\lambda_0)$, where λ_0 is the asymptotic wavelength, to be equal to -0.063. It is not clear how significantly this value differs from zero which it should be according to our equation (3.25). Another interesting result obtained in these works is the phenomenon of instability of straight filament with positive tension because of high twist rate. Obviously, such an instability cannot be described by equation (4.1). Keener & Tyson (1991) tried to describe it by invoking higher-order terms to the system (2.10)–(2.12). Another and, may be, more adequate way would be to derive dynamic equations valid for finite twist rates. Biktashev (1989*a*) has presented such an equation for a straight filament.

The numerical experiments presented in this paper, show that in simple cases, the behaviour of scroll waves can be understood in terms of equations (3.26)–(3.28), and, in particular, the prediction about monotonicity of filament length rate remains valid far beyond the formal limits of applicability of the asymptotic theory. The most interesting consequences has this property for filaments with negative tension, since it requires that the 'density of vortices' of the medium will grow until it will be stopped by other factors, such as interaction of vortices with boundaries or with each other. We have shown, for instance, that this pro-

PHILOSOPHICAL TRANSACTIONS OF THE ROYAL SOCIETY A MATHEMATICAL, PHYSICAL & ENGINEERING SCIENCES

cess can lead to multiplication of vortices. Note that this is an essentially three-dimensional effect, and such media may have no qualitatively peculiar properties in two dimensions.

The few known examples of excitable media with negative filament tension are all characterized by a low excitability of the medium and low wavefront velocities, both of which are associated with fibrillation in cardiac tissue. So, the behaviour of such vortices could provide a possible mechanism for the origin of fibrillation in cardiac tissue. This hypothetical scenario differs from other proposals (see Krinsky 1968; Holden *et al.* 1991; Holden 1994) in two key aspects: it does not depend on inhomogeneity of the medium, and it is essentially three dimensional. Further investigation of this phenomenon, and in particular, its relevance in cardiac pathology is needed.

As we mentioned above, chemical autowave media in a homogeneous phase usually have approximately equal diffusion coefficients, and for the case of equal diffusion coefficients the filament tension is always positive and equal to these diffusion coefficients. For this reason, the phenomenon of filament lengthening will not be observed in homogeneous chemical media. However, Agladze *et al.* (1992) have shown it is possible to obtain dramatically unequal diffusion coefficients in heterogeneous reaction media. Such media might provide an experimental testbed for exploring the essentially three dimensional phenomena associated with negative filament tension.

This work was supported in part by grants from Russian Fund for Fundamental Research no. 93-011-16080 (Pushchino) and Wellcome Trust 03881712, NATO CRG 920656 and SERC GR/J35641 (Leeds). The computations were performed on an Indigo^2 workstation and the Computationally Intensive Facility at Leeds University. The three-dimensional graphics were produced using a PC program written by V. N. Kochin and V. A. Kulikov (GeoGraph Software, Protvino, Russia), and using Explorer II on the Indigo^2. We are grateful to M. J. Poole for his help with networking and visualization. V.N.B. is thankful to V. Krinsky, A. Panfilov, A. Pertsov, E. Shnol, A. Winfree, anonymous referees and many other colleagues, for useful discussions and criticism concerning the analytical part of this paper.

Appendix A. Numerical methods

We use the cubic FitzHugh–Nagumo equations which takes the form

$$\partial_t u = \epsilon^{-1}(u - u^3/3 - v) + D\Delta_3 u, \quad \partial_t v = \epsilon(u + \gamma - \beta v), \tag{A 1}$$

where u is the excitation variable ('propagator'), v is the recovery variable ('controller'), D is the diffusion coefficient, ϵ, γ and β are constant parameters, and Δ_3 is the three-dimensional laplacian operator. In the paper, we refer to the the time and spatial coordinates of the model (A 1) as measured in time units (tu) and space units (su) respectively.

In numerical experiments, we take $D = 1$, $\gamma = 0.5$, $\epsilon = 0.3$ and solve (A 1) for two different values of parameter $\beta = 0.68$ and $\beta = 0.8$. The simulations are performed using the explicit Euler method with the simplest seven-point approximation of the laplacian operator, on a cuboidal lattice with space step 0.5 su and time step 0.03 tu. We use the non-flux boundary conditions $(\boldsymbol{n}\nabla)u\,|_\Gamma = 0$, where $\boldsymbol{n}$ is the normal vector to the boundary Γ. The choice of parameters was made based on the review of properties of the system (A 1) presented by Winfree (1991).

Initial conditions were typically constructed in the following way. First, in two-

dimensional experiments we determined the asymptotic wavelength of the spiral, inherent to the medium with the chosen parameters, and wrote the sequence of values that the variables u and v took in a point of the medium distant from core during one rotation period, and this sequence was used later as values of u, v at various phases. Then we prescribed a phase distribution in the three-dimensional medium according to the desired filament shape. To form this phase distribution, an Archimedean approximation of spiral shape was used, based on the asymptotic length λ determined from two-dimensional experiments. For instance, to form a vortex ring with centre at the origin, we prescribed the phase by the formula

$$\varphi(x,y,z) = 2\pi\rho(x,y,z)/\lambda + \psi(x,y,z), \tag{A 2}$$

where ρ, ψ, are two of the toroidal coordinates (ρ,ψ,θ) defined by equations

$$x = (R_\mathrm{f} + \rho\cos\psi)\cos\theta \quad y = (R_\mathrm{f} + \rho\cos\psi)\sin\theta \quad z = \rho\sin\psi, \tag{A 3}$$

and R_f is the radius of the circular filament. Based on this phase distribution, we assigned to each node of the grid the values of dynamic variables u, v, using linear interpolation from the sequence obtained in two-dimensional calculations. The vortex with straight filament can be constructed in the same way using the same formula (A 2) but with ρ, ψ being axial coordinates.

To present the form of the excitation wave, both two dynamic variables u and v were used (see figure 1, the first row). We displayed, for chosen time moments, the region where the excitation variable u is greater some threshold value, u_*, i.e. the current position of excitation wave; and we coloured this region depending on the values of the recovery variable v, which allows to distinguish front and back of the excitation wave.

For numerical extraction of the vortex filament, we use two different methods which create different geometrical objects based on the numeric solution of PDE. The first method extracts the core of the vortex which is defined as the region that was not excited during one rotation period of the vortex (figure 1, the last row). This method works well when the core of the vortex is thick enough and the vortex does not move too fast, so as its period is well defined. For the first reason, we used it only for the 'weak' media, with large core, which have negative tension of the filament.

Another approximation for the vortex filament is the line of phase singularity, or singular filament. Geometrically, it can be defined as the line obeying the equations

$$u(x,y,z) = u_* \quad v(x,y,z) = v_* \tag{A 4}$$

at properly chosen constants u_*, v_*. On the picture of excitation wave, this line corresponds to the line on the surface of the drawn region, where the dark shade changes to the light one, i.e. the edge between front and back of the excitation wave. A simple numerical procedure was used to extract the singular filament defined in this way. Namely, we took that a grid cell belongs to the filament if it has neighbouring grid nodes being in each of three different states:

$$\left.\begin{array}{ll} \text{(i)} & u < u_*, \quad v < v_*, \\ \text{(ii)} & u > u_*, \quad (u-u_*) > (v-v_*), \\ \text{(iii)} & v > v_*, \quad (u-u_*) < (v-v_*), \end{array}\right\} \tag{A 5}$$

The definition of singular filament has the advantage that it can be used for an

instant state of the medium, so it needs no additional memory for collecting information during the rotation period, and can be determined for any complicated excitation pattern. It has the disadvantage that the position of the singular filament oscillates with the vortex rotation (this is especially significant for the weak media; see figure 1) and this fact should be taken into consideration when analyzing the experimental results. The simplified version of this definitions we used, with determining just the 'singular grid cells', is simply realized and yields quite satisfactory results (figure 1, 2nd row). To diminish the value of the oscillations, on other figures we present patterns output synchronously with arrival of the excitation wave to a chosen piece of the medium, which in the case of sufficiently slow vortex drift, corresponds to the same rotation phase.

References

Agladze, K., Dulos, E., DeKepper, P. 1992 Turing patterns in confined gel and gel-free media. *J. phys. Chem.* **96**, 2400–2403.

Biktashev, V. N. 1989*a* Evolution of twist of an autowave vortex. *Physica* D **36**, 167–172.

Biktashev, V. N. 1989*b* Drift of a reverberator in an active medium due to interaction with boundaries. In *Nonlinear waves. II. Dynamics and evolution* (ed. A. V. Gaponov-Grekhov, M. I. Rabinovich & J. Engelbrecht), pp. 87–96. Springer Verlag.

Biktashev, V. N. & Holden, A. V. 1993 Resonant drift of an autowave vortex in a bounded medium. *Phys. Lett.* A **181**, 216–244.

Biktashev, V. N. & Holden, A. V. 1994 Resonant drift of autowave vortices in two-dimensional and the effects of boundaries and inhomogeneities. *Chaos, solitons and fractals.* (In the press.)

Brazhnik, P. K., Davydov, V. A., Zykov, V. S. & Mikhailov, A. S. 1988 Vortex rings in distributed active systems. *Sov. Phys. JETP* **93**, 1725.

Courtemanche, P. J., Skaggs, W. & Winfree, A. T. 1990 Stable three-dimensional action potential circulation in the FitzHugh–Nagumo model. *Physica* D **41**, 173–182.

Da Rios, L. S. 1906 Sul moto d'un liquido indefinito con un filetto vorticoso di forma qualinque. *Rend. Circolo Matematico Palermo* **22**, 117–135.

Davydov, V. A., Zykov, V. S., Mikhailov, A. S. & Brazhnik, P. K. 1988 Drift and resonance of spiral waves in distributed media. *Izv. Vuzov Radiofizika* **31**, 574–582.

Ermakova, E. A. & Pertsov, A. M. 1986 Interaction of rotating spiral waves with boundary. *Biofizika* **31**, 855–861.

Ermakova, E. A., Pertsov, A. M. & Shnol, E. E. 1989 On the interaction of vortices in two-dimensional active media. *Physica* D **40**, 185–195.

Henze, C., Lugosi E. & Winfree, A. T. 1990 Helical organizing centers in excitable media. *Can. J. Phys.* **68**, 683–710.

Holden, A. V., Markus, M. & Othmer, H. (eds) 1991 *Nonlinear wave processes in excitable media.* New York: Plenum.

Holden, A. V. (ed.) 1994 *Nonlinear phenomena in excitable physiological systems.* Proc. NATO ARW. Pergamon Press.

Hramov, R. N., Rudenko, A. N., Panfilov, A. V. & Krinsky, V. I. 1984 Drift of vortices in heterogeneous active medium (simplified analysis). *Studia Biophysica* **102**, 69–74

Janse, M. J. 1991 Reentrant arrhythmias. In *The heart and circulatory system,* 2nd edn (ed. H. A. Fozzard *et al.*), pp. 2055–2094. Raven Press.

Keener, J. P. 1988 The dynamics of three dimensional scroll waves in excitable media. *Physica* D **31**, 269–276.

Keener, J. P. & Tyson, J. J. 1988 The motion of untwisted untorted scroll waves in Belousov–Zhabotinsky reagent. *Science, Wash.* **239**, 1284–1286.

PHILOSOPHICAL TRANSACTIONS OF THE ROYAL SOCIETY A MATHEMATICAL, PHYSICAL & ENGINEERING SCIENCES

Keener, J. P & Tyson, J. J. 1990 Helical and circular scroll wave filaments. *Physica* D **44**, 191–202.

Keener, J. P. & Tyson, J. J. 1991 The dynamics of helical scroll waves in excitable media. *Physica* D **53**, 151–161.

Krinsky, V. I. 1968 Fibrillation in excitable media. *Problemy Kibernetiki* **20**, 59–80. (In Russian.)

Krinsky, V., Biktashev, V. N. & Pertsov, A. M. 1990 Autowave approaches to the cessation of autowave arrhythmias. *Ann. N.Y. Acad. Sci.* **591**, 232–246.

Krinsky, V. I., Pertsov, A. M., Fast, V. G. & Biktashev, V. N. 1991 A study of the autowave mechanisms of cardiac arrhythmias. In *Nonlinear wave processes in excitable media* (ed. A. V. Holden *et al.*), pp. 5–14. NATO ASI Series B, vol. 244 New York and London: Plenum.

Nandapurkar, P. J. & Winfree, A. T. 1989 Dynamical stability of untwisted scroll rings in excitable media. *Physica* D **35**, 277–288.

Panfilov, A. V. 1991 Three-dimensional vortices in active media. In *Nonlinear wave processes in excitable media* (ed. A. V. Holden *et al.*), pp. 361–382. NATO ASI Series B, vol. 244. New York and London: Plenum.

Panfilov, A. V., Aliev, R. R. & Mushinsky, A. V. 1989 An integral invariant for scroll rings in a reaction-diffusion system. *Physica* D **36**, 181–188.

Panfilov, A. V. & Holden, A. V. 1993 Computer simulation of re-entry sources in myocardium in two and three dimensions. *J. theor. Biol.* **161**, 271–285.

Panfilov, A. V. & Pertsov, A. M. 1984 Vortex rings in a three-dimensional active medium described by reaction-diffusion equations. *Dokl. Akad. Nauk.* **274**, 1500–1503. (In Russian.)

Panfilov, A. V. & Rudenko, A. N. 1987 Two regimes of the scroll ring drift in three-dimensional active media. *Physica* D **28**, 215–218.

Panfilov, A. V., Rundenko, A. N. & Pertsov, A. M. 1984 Twisted scroll waves in three-dimensional active media. In *Self-organization, autowaves and structures far from equilibrium*(ed. V. I. Krinsky), pp. 103–105. Berlin, Heidelberg, New York and Tokyo: Springer.

Panfilov, A. V., Rudenko, A. N. & Krinsky V. I. 1986 Vortex rings in three-dimensional active media with diffusion of two components. *Biofizika* **31**, 850–854. (In Russian.)

Panfilov A. V. & Vasiev, B. N. 1991 Vortex initiation in a heterogeneous excitable medium. *Physica* D **49**, 107–113.

Pertsov, A. M. & Ermakova, E. A. 1988 Mechanism of the drift of a spiral wave in an inhomogeneous medium. *Biofizika* **33**, 338–342.

Pismen, L. M. & Nepomnyashchy, A. A. 1991 Mobility of spiral waves. *Phys. Rev.* A **44**, 2243–2246.

Pismen, L. M. & Nepomnyashchy, A. A. 1992 On interaction of spiral waves. *Physica* D **54**, 183–193.

Ricca, R. L. 1991 Rediscovery of Da Rios equations. *Nature, Lond.* **352**, 561–562.

Ricca, R. L. 1992 Physical interpretation of certain invariants for filament motion under LIA. *Phys. Fluids* A **4**, 938–944.

Rudenko, A. N. & Panfilov, A. V. 1983 Drift and interaction of vortices in a two-dimensional inhomogeneous active medium. *Studia Biophysica* **98**, 183–188.

Vinson, M., Pertsov, A. & Jalife, J. 1993 Anchoring of vortex filaments in three-dimensional excitable media. *Physica* D. (In the press.)

Winfree, A. T. 1973 Scroll-shaped waves of chemical activity in three dimensions. *Science, Wash.* **181**, 937–938.

Winfree, A. T. 1990 Stable particle-like solutions to the nonlinear wave equations of three-dimensional excitable media. *SIAM Rev.* **32**, 1–53.

Winfree, A. T. 1991 Varieties of spiral wave behaviour – an experimentalist's approach to the theory of excitable media. *Chaos* **1**, 303–334.

Yakushevich, L. V. 1984 Vortex filament elasticity in active medium. *Studia Biophysica* **100**, 195–200.

PHILOSOPHICAL TRANSACTIONS OF THE ROYAL SOCIETY A MATHEMATICAL, PHYSICAL & ENGINEERING SCIENCES